A spatial genomic approach identifies time lags and historic barriers to gene flow in a rapidly fragmenting Appalachian landscape

Running title: Spatial genomics and historic fragmentation

Thomas A. Maigret[1,2]*, **John J. Cox**[2], **and David W. Weisrock**[1].

[1]University of Kentucky, Department of Biology, Lexington, KY 40506

[2]University of Kentucky, Department of Forestry and Natural Resources, Lexington, KY 40506

***corresponding author, thomas.maigret@uky.edu**

Abstract: The resolution offered by genomic data sets coupled with recently developed spatially informed analyses are allowing researchers to quantify population structure at increasingly fine temporal and spatial scales. However, uncertainties regarding data set size and quality thresholds and the time scale at which barriers to gene flow become detectable have limited both empirical research and conservation measures. Here, we used restriction site associated DNA sequencing to generate a large SNP data set for the copperhead snake (*Agkistrodon contortrix*) and address the population genomic impacts of recent and widespread landscape modification across an approximately 1000 km^2 region of eastern Kentucky. Nonspatial population-based assignment and clustering methods supported little to no population structure. However, using individual-based spatial autocorrelation approaches we found evidence for genetic structuring which closely follows the path of a historic highway which experienced high traffic volumes from ca. 1920 to 1970. We found no similar spatial genomic signatures associated with more recently constructed

highways or surface mining activity, though a time lag effect may be responsible for the lack of any emergent spatial genetic patterns. Subsampling of our SNP data set suggested that similar results could be obtained with as few as 250 SNPs, and thresholds for missing data exhibited limited impacts on the spatial patterns we detected outside of very strict or permissive extremes. Our findings highlight the importance of temporal factors in landscape genetics approaches, and suggest the potential advantages of large genomic data sets and fine-scale, spatially-informed approaches for quantifying subtle genetic patterns in temporally complex landscapes.

Key words: copperheads, landscape genomics, road ecology, mountaintop mining, ddRAD

Introduction

Habitat loss and fragmentation resulting from natural resource extraction, agriculture, and urbanization is setting some populations on new demographic trajectories, with increasing and persistent genetic diversity loss (Haddad et al. 2015). Understanding the effects of this rapid landscape change on population structure and genetic diversity is critical for informing science-based conservation and management (Hilty et al. 2012, Keller et al. 2015, Waits et al. 2016). However, a variety of geographic and ecological factors can affect the amount and rate at which spatial genetic structuring builds in a given system, creating challenges for the development of proactive management plans (Epps and Keyghobadi 2015, Balkenhol et al. 2016, Richardson et al. 2016). Thus, while migration may be limited by contemporary landscape factors, genetic structure may not be detectable until many generations after a barrier forms, especially if the power to detect such patterns is limited by the quantity or quality of genetic data available (Landguth et al. 2010, McCartney-Melstad et al. 2018).

The use of large single nucleotide polymorphism (SNP) data sets has improved the detection of recent habitat fragmentation in several ways. First, increased genome-wide sampling reduces the number of individuals needed to quantify differentiation among sampling locations (Willing et al. 2012, Nazareno et al. 2017). With this lower threshold for per-locale individual sampling, genomic data can permit sampling schemes encompassing a broader geographic area and a more hierarchical design, thus allowing for more robust resolution of patterns at multiple spatial scales (Anderson et al. 2010, Balkenhol and Fortin 2016). Furthermore, while the relatively high mutation rate of microsatellites is advantageous for detecting recent genetic change (Epps and Keyghobadi 2015), the greater genome-wide sampling of large SNP data sets can potentially detect weaker spatial genetic patterns resulting from relatively recent or porous

barriers to gene flow (Landguth et al. 2012). For example, McCartney-Melstad et al. (2018) found that with as few as 300-400 SNPs, genetic structure associated with the barrier effects of roads could be detected in amphibian populations where 12 microsatellite loci had previously indicated no structure. SNP data sets of this size are now readily available through methods such as restriction site-associated DNA sequencing (RADseq), allowing for the generation of thousands of loci from non-model organisms with a range of ecological characteristics that may make them prone to the genetic effects of recent habitat fragmentation (Epps and Keyghobadi 2015).

While traditional methods of testing for spatial genetic patterns, such as model-based clustering (e.g., STRUCTURE, Pritchard et al. 2000) or non-parametric exploratory data analyses (e.g., DAPC, Jombart et al. 2010), have been used to characterize genetic diversity across a given area (François and Waits 2015), other methods which are able to separate spatial and non-spatial genetic variation may be better equipped to detect patterns of genetic differentiation in recently fragmented systems or those with high rates of gene flow (Jombart et al. 2008, Galpern et al. 2014). These methods use spatial autocorrelation to tease apart patterns of inter- versus intra-population genetic variation, improving the identification of population structure at fine geographic scales (Galpern et al. 2012). When coupled with genomic data, spatially-informed analyses may also allow for the detection of weak spatial structure related to recent habitat fragmentation or incomplete barriers to migration (Richardson et al. 2016, Richardson et al. 2017, Combs et al. 2018, Combs et al. 2018a). However, alongside these methodological improvements, work remains to understand the amount of genomic data necessary to assess spatial genetic patterns (e.g., McCartney-Melstad et al. 2018), and the effects of genomic data quality on the resolution of recently evolved population structure.

Identifying spatial genetic patterns associated with landscape features is especially pertinent in regions experiencing rapid and recent landscape change. Few regions have experienced this change as rapidly as central Appalachia in the eastern United States, chiefly as a result of the large-scale surface coal mining practices often referred to as 'mountaintop removal' (Wickham et al. 2007, Drummond and Loveland 2010, Pericak et al. 2018, Maigret et al. 2019). Alongside mining, the wholesale construction of several high-traffic road systems in the 1970s and 1980s, in part to facilitate the transportation needs of the mining sector, have further subdivided what was formerly a relatively continuous forest landscape with scant high-traffic roads (KTC 2018). Despite the scale of these changes, the effects on native biodiversity are not well understood (Wickham et al. 2013). Given the historically rugged terrain of Appalachia, topographic homogenization produced by surface mining may facilitate dispersal of terrestrial fauna not encumbered by the radically altered soils, flora, and thermal regimes of reclaimed minelands (Wickham et al. 2013), and highways may also facilitate movement in some species (Trombulak and Fissell 2000). Alternatively, less vagile taxa that rely on sparsely distributed microhabitats may be more sensitive to the effects of forest fragmentation, especially if they are susceptible to road mortality.

We sought to understand the impact of recent and major landscape changes on the population structure of the copperhead (*Agkistrodon contortrix*), an abundant snake in eastern Kentucky (Barbour 1962) generally not capable of long-distance (> 1km) individual movements (Sutton et al. 2017). Copperheads rely on rocky hibernacula located high on steep-sided, south-facing slopes for overwintering (Maigret and Cox 2018), sites disproportionately destroyed by surface mining (Maigret et al. 2019). Copperheads are also generally intolerant of dense, invasive vegetation common to many reclaimed surface mines (Carter et al. 2015, Carter et al.

2017). Additionally, herpetofauna generally, and pit vipers in particular, have been shown to be especially vulnerable to vehicular traffic (Andrews and Gibbons 2005, Shepard et al. 2008), and elevated genetic differentiation associated with highways has been detected using microsatellite markers (Clark et al. 2010, DiLeo et al. 2013). Pertinent to this point, our study area contains several major highways [> 3,000 Annual Average Daily Traffic (AADT)] constructed between 1970 and 1985 which could be barriers to movement for *A. contortrix*. Nearly all these highways were constructed along new paths and do not follow major hydrological or topographic features for the majority of their route through the study area. From at least 1900 until 1970, however, the only highway across the study area was KY State Route 476 (formerly old KY State Route 15; hereafter referred to as KY-476). Prior to 1970, KY-476 was a major thoroughfare through the region, following the sinuous course of Troublesome Creek, a tributary of the North Fork of the Kentucky River. This constrained vehicle speed and made the route prone to frequent flood damage, prompting the development and opening of the new KY-15 c. 1975, leading to markedly decreased traffic volumes on KY-476 (~500 vehicles/day) and pushing most traffic, including many coal-industry commercial vehicles to the new KY-15 (~ 5,000 vehicles/day).

Using RADseq data and nonspatial and spatially informed analyses, we investigated the potential for recently formed population structure across *A. contortrix* in eastern Kentucky as a result of this landscape change, with a particular focus on the effects of habitat fragmentation via surface coal mining and through the network of historic (c. 1920) and more recently-constructed (c. 1975) high-traffic roads. Specifically, we aimed to: (1) understand the extent and scale of spatial genomic structuring in copperheads across what was until recently a heavily forested landscape; (2) test for associations between current landcover classes and patterns of spatial genomic diversity; (3) identify current or historic linear landscape features which are associated

126 with reduced gene flow, and (4) understand how the size and quality of a data set can affect our
127 ability to detect spatial genomic patterns. More broadly, we aim to shed light on the temporal
128 scale at which barriers to gene flow are detectable using large SNP data sets, to investigate the
129 potential role of spatially-informed methods for identifying recent or weak genetic boundaries,
130 and to provide a starting point for future research into the spatial genetic implications of
131 increasingly popular methods of surface mining.
132
133 **Methods**
134
135 2.1 *Sampling methods*
136 We sampled *A. contortrix* individuals from an approximately 1,000 km^2 area of Breathitt,
137 Knott, and Perry counties in eastern Kentucky, USA (Figure 1). We used a hierarchical sampling
138 strategy, sampling at arrays of four to six individual capture sites (Figure 1A). Each individual
139 capture site consisted of a location where a combination of artificial cover and visual encounter
140 surveys were used to capture snakes. An array was composed of at least four individual capture
141 sites, separated by 2-3 km, and arranged roughly in a cross or an 'x'. In turn, each array was
142 separated by roughly 10-20 km, providing comparisons at multiple spatial scales both within and
143 between each array (Balkenhol and Fortin 2016). Between May 2014 and September 2016,
144 individuals were captured at sampling sites, typically under artificial cover (e.g., sheet metal or
145 other debris). We augmented this design by including individuals captured apart from designated
146 individual capture sites; typically, these snakes were found alive or dead on roadways within the
147 study area or were killed and/or donated by area residents who were able to provide precise
148 locality information for each tissue sample. Live-captured snakes were restrained and two ventral

149 scales were removed, placed in 95% ethanol, and subsequently frozen at -80°C (Maigret 2019).
150 Muscular tissue from the tails of dead snakes was treated similarly.
151
152 2.2. *DNA sequencing and SNP calling*
153 We extracted genomic DNA using a Qiagen DNeasy Blood and Tissue Extraction Kit
154 and prepared double digest RADseq (ddRADseq) libraries based on Peterson et al. (2012). DNA
155 was quantified using a Qubit 2.0 flourometer (Thermo-Fisher). DNA extractions ≤ 2.0 ng/uL
156 were amplified using a Qiagen REPLI-g high-fidelity whole genome amplification kit. We
157 prepared ddRADseq libraries using ~1000 ng of DNA per individual. DNA was digested using
158 EcoRI and SphI and subsequently cleaned with Agencourt Ampure XP beads (Beckman
159 Coulter). Adaptor ligation was performed using one of 48 unique 5 bp barcodes in combination
160 with a universal 6 bp single-index PCR adaptor. Samples were then pooled in groups of 8, bead
161 cleaned, and size selected (526 bp ± 10%) with a Pippin Prep (Sage Science). Each 8-sample
162 pool was then Qbit quantified and amplified using Phusion high-fidelity PCR (New England
163 Biolabs) with a PCR primer with one of three unique barcodes, permitting each individual to be
164 identified uniquely using a combination of the unique PCR barcode and a unique adaptor index.
165 After cleaning and quantifying PCR product, we used an Agilent 2100 Bioanalyzer to confirm
166 target fragment size distributions before 150 bp paired-end sequencing on two lanes of an
167 Illumina Hi-Seq 2500. Individuals were randomly assigned to a lane with respect to geographic
168 location to reduce downstream genetic artefacts (Meirmans 2015).
169 We used Stacks v1.37 (Catchen et al. 2013) to identify orthologous loci across
170 individuals. No overlap was expected between sequencing reads; therefore, we used a custom
171 script to stitch together forward and reverse reads. We used process_radtags to demultiplex

172 individuals and discard low-quality reads containing uncalled bases or a mean quality score < 10
173 in a sliding window comprising 15% of the read. After quality filtering, reads were assembled
174 using denovo_map, with a minimum stack depth of 5 (m = 5), 3 mismatches allowed between
175 stacks within individuals (M = 3), and 2 mismatches allowed between stacks among individuals
176 (n = 2). To increase confidence in our SNP calls, we used rxstacks to remove SNPs with a low
177 log likelihood (--ln_lim = -25) and/or a high proportion of confounded loci (conf_lim = 0.25).
178 After running rxstacks, cstacks and sstacks were re-run with the filtered loci. We sampled a
179 single SNP per locus (--write-single-snp), using only SNPs with < 50% missing data, a minor
180 allele frequency < 0.015, and no evidence of excess heterozygosity. Finally, we removed
181 individuals with > 50% missing data.
182
183 2.3 *Summary statistics and distance-based analyses*
184 We generated a genetic dissimilarity matrix using the program bed2diffs v1 in the EEMS
185 package (Petkova et al. 2016). This produced a matrix of average individual pairwise genetic
186 dissimilarity (hereafter referred to as the "GDM") based on allelic frequencies, similar to the
187 proportion of shared alleles (Bowcock et al. 1994). We estimated effective population size using
188 the linkage disequilibrium method in NeEstimator (Do et al. 2014). We estimated heterozygosity
189 and nucleotide diversity using plink and vcftools, respectively (Purcell et al. 2007, Danecek et al.
190 2011). We calculated the relationship between geography and the GDM using the ecodist
191 package in R. Mantel correlograms were generated for multiple geographic distances, including
192 Euclidean distance, the natural log of distance, stream (hydrological) distance, and the natural
193 log of stream distance. To quantify stream distances, we used the Origin-Destination Cost Matrix
194 tool in ArcMap v10.1 (ESRI, Redlands, CA) and a shapefile of USGS stream paths obtained

195 from the KY Division of Geographic Information. We chose to use stream paths as a proxy for
196 potential elevation effects given the rugged terrain of the study area.
197
198 2.4 *Nonspatial analyses of population structure*
199 To identify and characterize genetic clusters across our study area, we used both
200 discriminant analysis of principal components (DAPC) in the adegenet R package (Jombart et al.
201 2010) and Bayesian clustering via STRUCTURE (Pritchard et al. 2000). For our DAPC analyses,
202 we first used the find.clusters function, retaining all principal components (PCs) and selecting
203 the *K* value with the lowest Bayesian information criterion (BIC). Individuals were then
204 ordinated in PC space using the dapc function. To reduce the potential for over-fitting, we
205 selected the number of retained PCs in light of diminishing returns from retaining excess PCs
206 (Jombart et al. 2010).
207 For our STRUCTURE analyses, we estimated population assignment of individuals using
208 an admixture model with cluster numbers ranging from $K = 1$ to 10. Five replicates were run for
209 each *K*, each for 1,000,000 generations after a burn-in of 100,000 generations. We used Structure
210 Harvester v0.6.9.4 (Earl and von Holt 2012) to generate mean log likelihood values for each *K*
211 and identify the optimal number of clusters for our data using ΔK (Evanno et al. 2005). We used
212 the program CLUMPAK to compute cluster membership coefficients across replicates (Kopelman
213 et al. 2015).
214
215 2.5 *Spatially informed analyses of population structure*
216 To further test for genetic structure across our study system, we used three recently
217 developed approaches that integrate spatial information into analyses based on genetic

dissimilarity. First, we used MEMGENE (Galpern et al. 2014), a regression-based analysis based on the spatial autocorrelation among a given set of georeferenced individuals and a corresponding GDM. Individual samples are mapped based on geographic location, and significant eigenvector scores are overlaid to provide a visualization of the geographic nature of genetic dissimilarity among individuals.

Second, we used the program sPCA (Jombart et al. 2008) implemented in the R package adegenet. sPCA is broadly similar to MEMGENE (but see Galpern et al. 2014:Appendix S4), but relies on an ordination approach based on Moran's *I* index to identify eigenvectors which maximize variation in allele frequencies and spatial autocorrelation, and then maps these eigenvectors on to geographic coordinates. Our analyses used a nearest-neighbor connection network with k = 40 neighbors to maximize potential connectivity across our large number of spatially distinct samples. We relied on the eigenvalue variance and spatial components plots to select the optimal number of global and local axes to retain, and used the recommended multivariate significance test to identify significant global and local genomic structure.

Third, to take into consideration the impact of landscape features on gene flow, we estimated a resistance model using the R package ResistanceGA (Peterman 2018). ResistanceGA uses a genetic algorithm approach to optimize the individual resistance values associated with a given resistance surface based on genetic dissimilarity data. Model fit of the optimized surfaces are quantified using AIC values from linear mixed-effects models, both for each surface individually and for all combinations of individual surfaces. Thus, ResistanceGA bypasses the often-subjective expert opinion parameterization stage of resistance surface construction (Spear et al. 2016, Peterman et al. 2018). Our ResistanceGA input landscape surfaces consisted of land cover classification data obtained from 2011 National Land Cover Data. We reclassified raw

241 NLCD raster values into 3 different resistance surfaces of two categories each, including: (1) a
242 mining surface with two categories, mined and unmined land, (2) a surface representing the route
243 of current highways, with two categories, highway and non-highway, and (3) a surface
244 representing the route of KY-476, also with two categories, highway and non-highway (Table
245 S1). We tested both for effects of each of these three surfaces independently and each possible
246 combination of the three. We reclassified NLCD raster classes using the Reclassify tool in the
247 Spatial Analyst extension of ArcMap 10.3.3, producing our three putative resistance surfaces.
248 We relied on historic road maps publicly available from the KY Transportation Cabinet to
249 identify current and historic highway patterns in the study area from 1936 to the present, and
250 historic topographic maps from the US Geological Survey's Historical Topographic Map
251 Explorer for information on routes before 1936. Our response data set was our individual
252 pairwise GDM, which we ran alongside our land cover raster surface using the 'costDistance'
253 function in the R package gdistance (van Etten 2017). This function calculates least cost paths
254 between each pair of locations, and while lacking the comprehensive approach available with
255 random walk commute times, least cost paths represent a much more computationally tractable
256 approach for our spatial and genetic data set (Peterman 2018).
257
258 2.6 *Subsampling of our SNP data set*
259 We aimed to assess the resolving power of two of the spatially informed methods, sPCA
260 and MEMGENE, based on: (1) the number of loci, and (2) the amount of missing data. To examine
261 the effect of the number of loci, we randomly subsampled our full 2,140 SNP data set, producing
262 subsets of 25, 50, 100, 250, 500, and 1,000 loci. For each subset, ten replicates were generated
263 using plink and analyzed in sPCA and MEMGENE as described above for the full data set. To

examine the effects of missing data, we re-filtered our raw SNP data set using missing data thresholds of 0.05 (i.e., retaining only loci present in ≥ 95% of individuals), 0.10, 0.25, 0.40, 0.5, 0.75, 0.90, and 0.95. While these represented our thresholds, our realized data sets typically had smaller amounts of missing data, in aggregate, than each threshold. Only a single data set could be produced for each missing data threshold.

Differences in the how sPCA and MEMGENE are designed influenced how we quantified our subsampling and missing data threshold results. For sPCA, we first detected significant patterns of structuring, then tabulated the proportion of replicates with unrelated, similar, or identical spatial genomic patterns as detected in analysis of the full data set. Model outputs for sPCA include global and local permutation tests of structuring, the p-values of which were obtained for each level of subsampling and missing data thresholds, which we averaged across ten replicates for the former. MEMGENE, on the other hand, only analyzes significant spatial patterns, and nonsignificant patterns are not retained for downstream analyses. Thus, for MEMGENE, we obtained R^2 values only for levels of subsampling and missing data thresholds where significant spatial patterns were observed, and we quantified spatial patterns which were unrelated, similar, or identical, in a similar fashion to our sPCA results. We visualized these results by charting p-values from local and global tests from sPCA alongside R^2 values from MEMGENE for each missing data threshold, and by charting both these statistical values and the proportion of similar patterns for each subsampling level. While categorizing spatial patterns in terms of their similarity to those generated using our full data set requires some qualitative assessment of the results, we chose not to use more substantial quantitative metrics for comparison (e.g., spatial point pattern analysis) given the limited number of sampling sites.

Results

3.1 *Sequencing results*

We generated ~239 million 150 bp paired-end reads, with a mean of 1,869,394 reads per individual. Increasing or decreasing the minimum read depth between 4 and 7 did not affect any summary statistics, and only marginally affected the number of loci in our data (Table S2). After filtering, we recovered genotypes for 77 individuals from 34 different locations (Figure 1). This included a total of 2,140 loci, with an average missing data rate of 23.5% of loci per individual (min. = 4.4%; max.= 48.9%).

3.2 *Summary of genetic diversity*

Across our study area, we estimated $H_O = 0.193$, $H_E = 0.24$, $\pi = 0.242$, and $F_{IS} = 0.195$. We estimated an N_e of 635.8 (95% CI: 595.6, 681.6). We identified weak, but sometimes significant correlations between genetic and different measures of geographic distances, including Euclidean ($p = 0.79$, $R^2 = -0.0003$), natural log of Euclidean ($p = 0.0006$, $R^2 = 0.0037$), hydrological distance ($p < 0.0001$, $R^2 = 0.0054$), and natural log of hydrological distance ($p = 0.003$, $R^2 = 0.0029$). Mantel correlograms of correlation by distance class similarly showed minimal evidence of isolation-by-distance (Figure S1).

3.3 *Non-spatial population structure*

Neither DAPC nor STRUCTURE analyses supported the presence of multiple geographically distinct genetic clusters. BIC scores in DAPC were lowest for $K = 1$ (Figure 2a), and an exploration of cluster assignments using the first PC axis and a $K = 2$ did not produce

individual assignments corresponding to sampling localities or geography. STRUCTURE analyses identified a $K = 3$ as the best-fit clustering model for our data based on the ΔK statistic (Figure 2b). However, at this level of clustering all individuals were nearly equally assigned to all three clusters, indicating a lack of population structure; these results were similar at a $K = 2$.

3.3 *Spatially informed population structure*

sPCA analyses identified significant global structure across the study area ($p = 0.002$). The first global (positive) sPCA axis identified a population genetic break that closely followed the path of KY-476 (Figure 3a). Based on a scree plot and a plot of eigenvalues, this first global axis contained the most information relative to other axes, and support for any of the local (negative) axes was not of congruent strength (Figure S2a-b).

The first variable identified as significant in the MEMGENE analysis explained a high proportion of the total variance across three retained axes (0.81). The proportion of overall genetic variance explained by spatial patterns associated with this first variable was modest (adj. $R^2 = 0.061$), yet was similar to the proportion explained by other studies at similar spatial scales (Galpern et al. 2014, Combs et al. 2018a). Visualization of the first and most explanatory MEM variable similarly identified a genetic break that partitioned populations on either side of KY-476 (Figure 3b). No genetic breaks identified an influence of landcover or current highway paths.

Landscape resistance analyses in ResistanceGA supported a null model of no geographic structure, followed by a model of isolation by distance (Tale S3). Models that included the three individual resistance surfaces (landcover, current highways, or historic highways), or any combination of resistance surfaces, were not strongly supported.

3.4 *Subsampling of SNP data set*

sPCA analysis of subsampled SNP data sets produced significant detection of global structure with as few as 25 loci (average global p-value of ten replicates = 0.067, Fig. 4a), although data sizes ≥ 250 loci were needed to produce identical patterns to those generated with the full data set (mean global p = 0.0033). At ≥ 500 loci identical patterns were produced in all replicates. Significant local structure was not supported for any level of subsampling (mean local p-value = 0.34). MEMGENE analysis of subsampled SNP data sets produced identical patterns in a majority of replicates when sampling ≥ 100 loci (Fig. 4b). However, identical results were still detected in 50% of replicates when sampling 50 loci and produced in all replicates when sampling 1000 loci.

The performance of sPCA and MEMGENE was not adversely affected by the inclusion of higher levels of missing data (Fig. 4c). Global p-values from sPCA analysis were significant at ≥ 25% missing data and remained so, even when the data set allowed for as much as 95% missing data per individual. Missing data levels ≤ 10% resulted in a loss of significant global spatial structure, and we note the peculiarity that data sets of smaller locus number resulted in significant detection of global structure in our subsampled data replicates, suggesting the potential for Type I error with small data sets. Non-zero R^2 estimates were produced in MEMGENE analyses of data sets permitting ≥ 40% missing and increased with higher levels of missing data, up to 75%.

Discussion

Non-spatial vs. spatially informed inference of population structure

Here, we present empirical evidence for the ability of some spatially informed methods to detect weak population structure in study systems where more traditional and non-spatially informed methods indicate a lack of structure. Patterns in both DAPC and Structure results were consistent with a $K = 1$ model, with no evidence for geographically distinct genetic clusters across the study area. In contrast, the spatially informed methods sPCA and MEMGENE returned similar results supporting geographic genetic structure with a break coinciding with the path of KY-476, a historically-important highway that served as a major traffic artery in the region between c. 1920-1975. The inference of weak population structure and genetic fragmentation on the landscape of our study system is bolstered by multiple lines of evidence. First, both sPCA and MEMGENE identified the same geographic genetic break. While these methods both use spatial autocorrelation in the analysis of genetic data, they operate in very different ways: sPCA relies on the integration of Moran's I matrix via a connection network, while MEMGENE uses a forward selection method to identify significant MEM eigenvectors, and then uses a regression approach to generate output variables which contain the spatial patterns (Galpern et al. 2014). The congruence of these results indicates that our result is probably not a spurious pattern driven by an artefact of one particular analysis. Second, while the magnitude of population structure detected in our work was generally weak— MEMGENE-based regression analyses attributed ~6% of total genetic variation to spatial effects—this amount of spatially explained genetic variation is in the range of that detected with MEMGENE under simulated models of population fragmentation and higher than that detected for panmictic populations (Galpern et al. 2014). This level of spatially driven genetic variation is also similar to that detected in other studies of recently fragmented landscapes (Combs et al. 2018a, Combs et al. 2018b). Our overall interpretation of these results is that the use of methods that specifically use spatial patterns of

379 variation, such as sPCA and MEMGENE, seem to be able to identify patterns of weak population
380 structure at temporal and spatial scales where more widely used non-spatial methods would fail
381 to discern geographic population structure (Galpern et al. 2014).

382 In contrast, our estimates of population structure using optimized landscape resistance
383 generated using ResistanceGA did not support a link between genetic differentiation and
384 landscape features. This lack of spatially informed population structure may be related to
385 methodological aspects of this program, as it does not use the autocorrelation approach that is
386 built in to sPCA and MEMGENE. In addition, our analyses were limited to only analyzing least
387 cost paths. ResistanceGA does allow for a more exhaustive exploration of restricted gene flow
388 across the landscape using a random-walk framework, which may have identified fragmentation
389 associated with landscape features that were not examined using a least cost path approach.
390 However, this required a computationally prohibitive set of analyses given our level of locality
391 sampling and landcover data resolution. Coupled with the relatively weak nature of the spatial
392 genomic signal associated with the route of KY-476, our ability to detect resistance to gene flow
393 based on landcover classes may have been comparatively limited.

394

395 *Data size and quality in the detection of weak population structure*

396 While our large genomic data set may have also increased our ability to detect subtle
397 spatial patterns, random subsampling of our data indicated that thousands of SNPs may not be
398 necessary to detect weak population structure similar to that found with our full data set. In fact,
399 we found that several hundred SNPs may be sufficient to consistently identify weak spatial
400 structure. This result is similar to that of a recent study (McCartney-Melstad et al. 2018), which
401 showed that the use of a more limited set of independent SNPs (~300-400) was sufficient to

recover fine-scale population structure using the non-spatial method Admixture (Alexander et al. 2009) with results similar to those obtained with a larger, more-complete data set (3095 SNPs). Our subsampling work extends this finding, indicating that spatially informed methods of population structure may be equally efficient with relatively modest sized data sets (~250-500 loci). We do note that minimum locus thresholds will vary based on the intensity of the spatial genetic signal, the number of individuals sampled, and a variety of other factors. However, these developing empirical findings provide an optimistic outlook on the minimum data size required for the detection of weak landscape-level fragmentation.

Our exploration of the inclusion of missing data yielded similarly optimistic results, where, under a wide range of thresholds, missing genotypes did not substantially alter our spatial landscape genomic findings. Using stringent missing genotype thresholds, which also lowered the number of SNPs in the data, actually decreased the spatial signal. Conversely, allowing for more missing data increased the signal of population structure in our data, with a plateau in the level of significance (sPCA) and amount of spatial variation explained (MEMGENE). The effect of missing data in population and evolutionary studies has seen mixed results. Simulation-based results have indicated that missing genotypes in RADseq data can result in substantial biases in a range of population genetic summary statistics, including F_{ST} (Arnold et al. 2013). In contrast, the use of more liberal missing data thresholds in RADseq-based phylogenetic studies has provided opportunities to recover phylogenetic patterns not detected using more stringent thresholds (Wagner et al. 2013, Eaton et al. 2017; but see Leaché et al. 2015). This may be due to a bias whereby loci with higher mutation rates, but likely to contain population or phylogenetic information, are eliminated by stringent missing thresholds (Huang and Knowles 2014). The effect of missing data in landscape genomic studies has yet to be thoroughly explored, and we

425 suggest based on our results that some spatially informed analyses may be robust to the recovery
426 of patterns of weak population structure despite the inclusion of a high level of missing
427 genotypes, but that parameter estimation at this geographic scale (e.g., migration rates) may be
428 more strongly influenced. Therefore, when possible, we second the recommendation of others
429 (Wagner et al. 2013, O'Leary et al. 2018) for researchers to explore the sensitivity of their results
430 across a range of different missing data thresholds.
431
432 *Copperhead landscape genomics and temporal considerations*
433 Our results further emphasize an association between high-traffic roads and genetic
434 differentiation in pit vipers (Clark et al. 2010, DiLeo et al. 2010, DiLeo et al. 2013, Bushar et al.
435 2015, Herrmann et al. 2017, but see Weyer et al. 2014). These findings are in addition to field
436 studies that have suggested the outsized role played by road mortality in snakes, and
437 herpetofauna more generally (Andrews and Gibbons 2005, Row et al. 2007, Shepard et al. 2008).
438 Furthermore, our results suggest that the effects of high-traffic roads and associated intense
439 human activity might persist for decades after traffic volumes decline, in line with predictions
440 from simulations (Landguth et al. 2010).
441 We did not find evidence for a strong influence of surface coal mining on genetic
442 connectivity, which was surprising given the widespread nature of surface mining in the study
443 area, and the wholesale shifts in vegetation, soils, topography, and fauna that characterize the
444 mining and mine reclamation process. Surface mining of coal in Appalachia has a high degree of
445 spatial and temporal variance; portions of mines can exist in various states of reclamation from
446 barren rock to early successional forest, and mining activity can cease for months to years as a
447 result of fluctuating coal prices or labor disputes, thus providing opportunities for animals to

maintain genetic connectivity in these novel landscapes. Regardless, we recommend further research into this generally understudied area, as the large scale and radical impacts of this mining practice may well result in detectable impacts in populations of other taxa (Wickham et al. 2013). This may be especially true for species with shorter generation times, smaller population sizes, and more exclusive associations with ridgetop forests (Epps and Keyghobadi 2015, Maigret et al. 2019).

We note that the connection between the identified genetic fragmentation and the historic highway KY-476 is a largely qualitative assessment, and several specific caveats deserve mention. The route of KY-476 corresponds not only to a highway path, but also to a swath of comparatively higher historic human population density and also to the route of Troublesome Creek, either of which could be factors more important than the highway itself. While modeling relative contributions of population density and road mortality is beyond the scope of our study, in terms of parallel geomorphology and hydrology, the historic highway path does not correspond to any major feature which might be expected to seriously reduce movement of copperheads (Figure S3). Other waterways which divide our sampling locations, including Lost Creek and Buckhorn Creek, are of similar size to Troublesome Creek. Moreover, copperheads and other pit vipers regularly cross bodies of water (T. Maigret, unpublished data; Clark et al. 2010), and studies have found that even hydropower reservoirs are ineffective barriers to gene flow in copperheads and similar species (Oyler-McCance and Parker 2010, Levine et al. 2016). More generally, a second caveat is that while we intended our sampling to be hierarchical in design, the broad scales at which genomic patterns exist in our study area means that we are examining a single functional landscape. When possible, landscape-scale replication would provide a more robust assessment of the effects of current and historic landscape features on

gene flow in *A. contortrix* and similar taxa (Short Bull et al. 2011). Moreover, assuming we have detected a spatial genomic pattern stemming from historic highway traffic, we have not determined the traffic threshold which would produce a noticeable spatial genetic pattern or the precise time lag which must pass before these patterns become detectable. Other research has suggested that even low amounts of traffic can produce genetic differentiation (Clark et al. 2010), and depending on a variety of demographic characteristics, numerous generations may need to pass before genetic differentiation becomes apparent (Landguth et al. 2010, Epps and Keyghobadi 2015). Thus, while we may have detected the effect of a historic roadway, we have not conclusively ruled out impacts of current roadways, or even low-traffic and unpaved county roads not included in our analysis. In a similar manner, our findings regarding the spatial genetic implications of surface mines should also be understood tentatively.

Our study adds to a growing list highlighting the potential for large SNP data sets to detect weak, recent, or otherwise subtle spatial genomic patterns (Gonzàlez-Serna et al. 2018, McCartney-Melstad et al. 2018, Murphy et al. 2018, Tan et al. 2018). Considering the problems time lags present for conservation planning, the use of large (> 250) SNP data sets and spatially informed analyses of genetic diversity will likely become increasingly important for placing patterns of population structuring in their proper genomic, temporal, and geographic contexts.

Data Accessibility

Sequence data, SNP calls, landcover rasters, and sample catalogs will be accessible upon acceptance via NCBI's sequence read archive (SRA) at accession number PRJNA6278371.

494 **Acknowledgements**

495 Our work was conducted under University of Kentucky Institutional Animal Care and Use
496 Committee (IACUC) Protocol 2012-0954. Funding was provided by a Theodore Roosevelt
497 Memorial Grant (American Museum of Natural History), McIntire Stennis Project KY009031
498 (US Department of Agriculture, National Institute of Food and Agriculture), a Kerri Casner
499 Environmental Sciences Fellowship (Tracy Farmer Institute for Sustainability and the
500 Environment), and an Ellers-Billing Award (University of Kentucky Appalachian Center). We
501 are grateful for field assistance provided by David Collett, Erwin Williams, Chris Osborne, Ted
502 Sizemore, Neva Williams, Grover Napier, RB Combs, Anthony Campbell, Scotty Brewer, Mark
503 Chaffins, Doran Howard, Taylor Hughes, Rudy Noble, Verle Fugate, the late Geraldine
504 McIntosh, and other residents of Breathitt, Perry, and Knott counties. We thank the University of
505 Kentucky's Center for Computational Sciences and Information Technology Services Research
506 Computing for use of the Lipscomb Computing Cluster resources. We are grateful for the
507 laboratory assistance of Nicolette Lawrence, Kara Jones, Mary Foley, and Ricky Grewelle.

508

List of Figures

Figure 1: Map of our study area and sampling localities superimposed over (A) the current and historic highway network, with sampling arrays (indicated with a-e) to which each sampling site belongs, and (B) landcover, including surface coal mines, forest, and other non-forest habitat.

Figure 2: Results of nonspatial population structure analyses, including (a) ΔK and individual assignment plots from Structure for $K = 3$ and $K = 2$, and (b) BIC and individual assignment plots from DAPC. Letters beneath each individual assignment plot correspond to the geographically distinct sampling arrays depicted in Figure 1a.

Figure 3: Results of our spatially informed population structure analyses. (a) Results of sPCA analyses visualized using interpolated vector scores, showing divergence coinciding with the historic highway path (designated in this study as KY-476), but not with landcover or current highway infrastructure. (b) Results of MEMGENE analysis, which suggests similar patterns of population structure associated with KY-476. Circle color and size represent the association and genetic similarity, respectively, along the first MEM variable axis.

Figure 4: Effects of the number of loci and missing data on (a) sPCA and (b) MEMGENE results, and the effects of missing data levels on both sets of results (c). For (a) and (b), the left y-axis represents the proportion of results which were identical, partially identical, or unrelated to the results obtained from the full data set depicted in Figure 3. Visualization results from each replicate are available in Figure S4. The right y-axis for (a) represents p-values from global and local tests for structuring.

Supplementary Material

Figure S1: Mantel correlograms for individual genetic differentiation versus (a) Euclidean distance, (b) natural log of Euclidean distance, (c) stream distance, and (d) natural log of stream distance. Filled circles represent significant values at $\alpha = 0.05$.

Figure S2: Eigenvalue plot (a) and scree plot (b) of local and global axes obtained from our sPCA analyses. The first global axis, in red, was the only axis retained, and displays unique separation from other potential axes in the scree plot (labeled as λ_1).

Figure S3: Digital elevation model of study area, with sample points corresponding to Figure 1.

Figure S4: Visualizations of results from each of the ten replicates for each random subset of loci, and each level of missing data. Includes (a) interpolated vector scores from sPCA, (b) plotted scores from sPCA, and (c) plotted MEM scores for significant results.

Table S1: Landcover reclassification scheme for our ResistanceGA resistance surface.

Table S2: Summary statistics for read depths from m = 4, m = 5, and m = 7.

553 **Table S3:** Model output from our ResistanceGA least-cost path analyses. A null model of no
554 geographic structure and a model of isolation-by-distance outperformed all combinations of
555 resistance surfaces based on historic roads, current roads, and surface mining.

556 **Literature Cited**
557
558 Alexander, D. H., Novembre, J., and Lange, K. 2009. Fast model-based estimation of ancestry in
559 unrelated individuals. Genome Research 19: 1655–1664.
560 Anderson, C.D., Epperson, B.K., Fortin, M.J., Holderegger, R., James, P.M., Rosenberg, M.S.,
561 Scribner, K.T. and Spear, S. 2010. Considering spatial and temporal scale in landscape-
562 genetic studies of gene flow. Molecular Ecology 19: 3565-3575
563 Andrews, K. M., and Gibbons, J. W. 2005. How do highways influence snake movement?
564 Behavioral responses to roads and vehicles. Copeia 2005: 772-782.
565 Arnold, B., Corbett-Detig, R. B., Hartl, D., and Bomblies, K. 2013. RADseq underestimates
566 diversity and introduces genealogical biases due to nonrandom haplotype sampling.
567 Molecular Ecology 22:3179–3190.
568 Balkenhol, N., and Fortin, M. J. 2016. Basics of study design: Sampling landscape heterogeneity
569 and genetic variation for landscape genetic studies. *In:* Landscape Genetics: Concepts,
570 Methods, Applications, First Edition. John Wiley and Sons Ltd., p. 58-76.
571 Balkenhol, N., Cushman, S. A., Waits, L. P., and Storfer, A. 2016. Current status, future
572 opportunities, and remaining challenges in landscape genetics. *In:* Landscape Genetics:
573 Concepts, Methods, Applications, First Edition. John Wiley and Sons Ltd., p. 247-255.
574 Barbour, R.W. 1962. An aggregation of copperheads, *Agkistrodon contortrix*. Copeia 1962: 640.
575 Bowcock, A. M., Ruiz-Linares, A., Tomfohrde, J., Minch, E., Kidd, J. R., and Cavalli-Sforza, L.
576 L. 1994. High resolution of human evolutionary trees with polymorphic microsatellites.
577 Nature 368: 455-457.
578 Bushar, L. M., Bhatt, N., Dunlop, M. C., Schocklin, C., Malloy, M. A., and Reinert, H. K. 2015.
579 Population isolation and genetic subdivision of timber rattlesnakes (*Crotalus horridus*) in
580 the New Jersey Pine Barrens. Herpetologica 71: 203-211.
581 Carter, E. T., Eads, B. C., Ravesi, M. J., and Kingsbury, B. A. 2015. Exotic invasive plants alter
582 thermal regimes: implications for management using a case study of a native ectotherm.
583 Functional Ecology 29: 683-693.
584 Carter, E. T., Ravesi, M. J., Eads, B. C., and Kingsbury, B. A. 2017. Invasive plant management
585 creates ecological traps for snakes. Biological Invasions 19: 443-453.
586 Catchen, J., Hohenlohe, P. A., Bassham, S., Amores, A., and Cresko, W. A. 2013. Stacks: an
587 analysis tool set for population genomics. Molecular Ecology 22: 3124-3140.
588 Clark, R. W., Brown, W. S., Stechert, R., and Zamudio, K. R. 2010. Roads, interrupted dispersal,
589 and genetic diversity in timber rattlesnakes. Conservation Biology 24:1059-1069.
590 Combs, M., Puckett, E.E., Richardson, J., Mims, D. and Munshi-South, J., 2018. Spatial
591 population genomics of the brown rat (*Rattus norvegicus*) in New York City. Molecular
592 Ecology 27: 83-98.
593 Combs, M., Byers, K.A., Ghersi, B.M., Blum, M.J., Caccone, A., Costa, F., Himsworth, C.G.,
594 Richardson, J.L. and Munshi-South, J., 2018a. Urban rat races: spatial population
595 genomics of brown rats (*Rattus norvegicus*) compared across multiple cities. Proceedings
596 of the Royal Society B: Biological Sciences 285: 20180245.
597 Danecek, P., Auton, A., Abecasis, G., Albers, C.A., Banks, E., DePristo, M.A., Handsaker, R.E.,
598 Lunter, G., Marth, G.T., Sherry, S.T. and McVean, G. 2011. The variant call format and
599 VCFtools. Bioinformatics 27: 2156-2158.
600 DiLeo, M. F., Row, J. R., and Lougheed, S. C. 2010. Discordant patterns of population structure
601 for two co-distributed snake species across a fragmented Ontario landscape. Diversity

602 and Distributions 16: 571-581.
603 DiLeo, M. F., Rouse, J. D., Dávila, J. A., and Lougheed, S. C. 2013. The influence of landscape
604 on gene flow in the eastern massasauga rattlesnake (*Sistrurus c. catenatus*): insight from
605 computer simulations. Molecular Ecology 22: 4483-4498.
606 Do, C., Waples, R.S., Peel, D., Macbeth, G.M., Tillett, B.J. and Ovenden, J.R. 2014.
607 NeEstimator v2: re-implementation of software for the estimation of contemporary
608 effective population size (Ne) from genetic data. Molecular Ecology Resources 14: 209-
609 214.
610 Drummond, M. A., and Loveland, T. R. 2010. Land-use pressure and a transition to forest-cover
611 loss in the eastern United States. BioScience 60: 286-298.
612 Earl, D. A., and von Holdt, B. M. 2012. STRUCTURE HARVESTER: a website and
613 program for visualizing STRUCTURE output and implementing the Evanno method.
614 Conservation Genetics Resources 4: 359-361.
615 Eaton, D. A. R., Spriggs, E. L., Park, B., and Donoghue, M. J. 2017. Misconceptions on missing
616 data in rad-seq phylogenetics with a deep-scale example from flowering plants.
617 Systematic Biology 66: 399–412.
618 Epps, C.W. and Keyghobadi, N. 2015. Landscape genetics in a changing world: disentangling
619 historical and contemporary influences and inferring change. Molecular Ecology 24:
620 6021-6040.
621 Evanno, G., Regnaut, S. and Goudet, J. 2005. Detecting the number of clusters of individuals
622 using the software STRUCTURE: a simulation study. Molecular Ecology 14:2611-2620.
623 François, O., and Waits, L. P. 2015. Clustering and assignment methods in landscape genetics.
624 *In:* Landscape Genetics: Concepts, Methods, Applications, First Edition. John Wiley and
625 Sons Ltd., p.114-128.
626 Galpern, P., Manseau, M. and Wilson, P. 2012. Grains of connectivity: analysis at multiple
627 spatial scales in landscape genetics. Molecular Ecology 21: 3996-4009.
628 Galpern, P., Peres-Neto, P. R., Polfus, J., and Manseau, M. 2014. MEMGENE: Spatial pattern
629 detection in genetic distance data. Methods in Ecology and Evolution 5: 1116-1120.
630 González-Serna, M. J., Cordero, P. J., and Ortego, J. 2018. Using high-throughput sequencing to
631 investigate the factors structuring genomic variation of a Mediterranean grasshopper of
632 great conservation concern. Scientific Reports 8: 13436.
633 Haddad, N.M., Brudvig, L.A., Clobert, J., Davies, K.F., Gonzalez, A., Holt, R.D., Lovejoy, T.E.,
634 Sexton, J.O., Austin, M.P., Collins, C.D., and Cook, W.M. 2015. Habitat fragmentation
635 and its lasting impact on Earth's ecosystems. Science Advances 1: e1500052.
636 Herrmann, H. W., Pozarowski, K. M., Ochoa, A., and Schuett, G. W. 2017. An interstate
637 highway affects gene flow in a top reptilian predator (Crotalus atrox) of the Sonoran
638 Desert. Conservation Genetics 18: 911-924.
639 Hilty, J. A., Lidicker Jr, W. Z., and Merenlender, A. 2012. Corridor ecology: the science and
640 practice of linking landscapes for biodiversity conservation. Island Press, Washington,
641 D.C., USA.
642 Huang, H., and Knowles, L. L. 2014. Unforeseen consequences of excluding missing data from
643 next-generation sequences: simulation study of RAD sequences. Systematic Biology 65:
644 357-365.
645 Jombart, T., Devillard, S., Dufour, A. B., and Pontier, D. 2008. Revealing cryptic spatial patterns
646 in genetic variability by a new multivariate method. Heredity 101: 92-103.
647 Jombart, T., Devillard, S., and Balloux, F. 2010. Discriminant analysis of principal components:

a new method for the analysis of genetically structured populations. BMC Genetics 11: 94.

Keller, D., Holderegger, R., van Strien, M. J., and Bolliger, J. 2015. How to make landscape genetics beneficial for conservation management? Conservation Genetics 16: 503-512.

Kentucky Transportation Cabinet [KTC]. 2018. Historical Maps: download archived county road aid maps. <https://transportation.ky.gov/Planning/Pages/Historical-Maps.aspx> Accessed 1 January 2019.

Kentucky Transportation Cabinet [KTC]. 2019. Interactive statewide traffic counts map. <https://transportation.ky.gov/Planning/Pages/Traffic-Counts.aspx> Accessed 30 January 2019.

Kopelman, N.M., Mayzel, J., Jakobsson, M., Rosenberg, N.A. and Mayrose, I. 2015. Clumpak: a program for identifying clustering modes and packaging population structure inferences across K. Molecular Ecology Resources 15: 1179-1191.

Landguth, E.L., Cushman, S.A., Schwartz, M.K., McKelvey, K.S., Murphy, M. and Luikart, G. 2010. Quantifying the lag time to detect barriers in landscape genetics. Molecular Ecology 19: 4179-4191.

Landguth, E.L., Fedy, B.C., Oyler-McCance, S.J., Garey, A.L., Emel, S.L., Mumma, M., Wagner, H.H., Fortin, M.J. and Cushman, S.A. 2012. Effects of sample size, number of markers, and allelic richness on the detection of spatial genetic pattern. Molecular Ecology Resources 12: 276-284.

Leaché, A.D., Banbury, B. L., Felsenstein, J., De Oca, A. N.-M., and Stamatakis, A. 2015. Short tree, long tree, right tree, wrong tree: new acquisition bias corrections for inferring snp phylogenies. Systematic Biology 64: 1032–1047.

Levine, B. A., Smith, C. F., Douglas, M. R., Davis, M. A., Schuett, G. W., Beaupre, S. J., and Douglas, M. E. 2016. Population genetics of the copperhead at its most northeastern distribution. Copeia 104: 448-457.

Maigret, T.A., and J.J. Cox. 2018. *Agkistrodon contortrix*: Hibernacula. Herpetological Review 49:123.

Maigret, T.A. 2019. Snake scale clips as a source of high-quality DNA suitable for RAD sequencing. Conservation Genetics Resources: in press.

Maigret, T.A., Cox, J.J., and J. Yang. 2019. Persistent geophysical effects of mining threaten ridgetop biota of Appalachian forests. Frontiers in Ecology and the Environment 17: 85-91.

McCartney-Melstad, E., Vu, J. K., and Shaffer, H. B. 2018. Genomic data recover previously undetectable fragmentation effects in an endangered amphibian. Molecular Ecology 27: 4430-4443.

Meirmans, P. G. 2015. Seven common mistakes in population genetics and how to avoid them. Molecular Ecology 24: 3223-3231.

Murphy, M. O., Jones, K. S., Price, S. J., and Weisrock, D. W. 2018. A genomic assessment of population structure and gene flow in an aquatic salamander identifies the roles of spatial scale, barriers, and river architecture. Freshwater Biology 63: 407-419.

Nazareno, A. G., Bemmels, J. B., Dick, C. W., and Lohmann, L. G. 2017. Minimum sample sizes for population genomics: An empirical study from an Amazonian plant species. Molecular Ecology Resources 17: 1136-1147.

O'Leary, S. J., Puritz, J. B., Willis, S. C., Hollenbeck, C. M., and Portnoy, D. S. 2018. These aren't the loci you're looking for: principles of effective SNP filtering for molecular

694 ecologists. Molecular Ecology 27: 3193-3206.
695 Pericak, A.A., Thomas, C.J., Kroodsma, D.A., Wasson, M.F., Ross, M.R., Clinton, N.E.,
696 Campagna, D.J., Franklin, Y., Bernhardt, E.S. and Amos, J.F. 2018. Mapping the yearly
697 extent of surface coal mining in Central Appalachia using Landsat and Google Earth
698 Engine. PloS one 13: e0197758.
699 Peterson, B. K., Weber, J. N., Kay, E. H., Fisher, H. S., and Hoekstra, H. E. 2012. Double digest
700 RADseq: an inexpensive method for de novo SNP discovery and genotyping in model
701 and non-model species. PloS one 7: e37135.
702 Peterman, W. E. 2018. ResistanceGA: An R package for the optimization of resistance surfaces
703 using genetic algorithms. Methods in Ecology and Evolution 9: 1638-1647.
704 Petkova, D., Novembre, J., and Stephens, M. 2016. Visualizing spatial population structure with
705 estimated effective migration surfaces. Nature Genetics 48: 94-100.
706 Pritchard, J. K., Stephens, M., and Donnelly, P. 2000. Inference of population structure
707 using multilocus genotype data. Genetics 155: 945-959.
708 Purcell, S., Neale, B., Todd-Brown, K., Thomas, L., Ferreira, M.A., Bender, D., Maller, J., Sklar,
709 P., De Bakker, P.I., Daly, M.J. and Sham, P.C. 2007. PLINK: a tool set for whole-
710 genome association and population-based linkage analyses. The American Journal of
711 Human Genetics 81: 559-575.
712 Richardson, J. L., Brady, S. P., Wang, I. J., and Spear, S. F. 2016. Navigating the pitfalls and
713 promise of landscape genetics. Molecular Ecology 25: 849-863.
714 Richardson, J.L., Burak, M.K., Hernandez, C., Shirvell, J.M., Mariani, C., Carvalho-Pereira,
715 T.S., Pertile, A.C., Panti-May, J.A., Pedra, G.G., Serrano, S. and Taylor, J. 2017. Using
716 fine-scale spatial genetics of Norway rats to improve control efforts and reduce
717 leptospirosis risk in urban slum environments. Evolutionary Applications 10: 323-337.
718 Row, J. R., Blouin-Demers, G., and Weatherhead, P. J. 2007. Demographic effects of road
719 mortality in black ratsnakes (*Elaphe obsoleta*). Biological Conservation 137: 117-124.
720 Shepard, D. B., Dreslik, M. J., Jellen, B. C., and Phillips, C. A. 2008. Reptile road mortality
721 around an oasis in the Illinois corn desert with emphasis on the endangered eastern
722 massasauga. Copeia 2008: 350-359.
723 Short Bull, R.A., Cushman, S.A., Mace, R., Chilton, T., Kendall, K.C., Landguth, E.L.,
724 Schwartz, M.K., McKelvey, K., Allendorf, F.W. and Luikart, G. 2011. Why replication
725 is important in landscape genetics: American black bear in the Rocky Mountains.
726 Molecular Ecology 20: 1092-1107.
727 Sutton, W. B., Wang, Y., Schweitzer, C. J., and McClure, C. J. 2017. Spatial ecology and multi-
728 scale habitat selection of the Copperhead (*Agkistrodon contortrix*) in a managed forest
729 landscape. Forest Ecology and Management 391: 469-481.
730 Tan, D.J., Chattopadhyay, B., Garg, K.M., Cros, E., Ericson, P.G., Irestedt, M. and Rheindt, F.E.
731 2018. Novel genome and genome-wide SNPs reveal early fragmentation effects in an
732 edge-tolerant songbird population across an urbanized tropical metropolis. Scientific
733 Reports 8: 12804.
734 Trombulak, S. C., and Frissell, C. A. 2000. Review of ecological effects of roads on terrestrial
735 and aquatic communities. Conservation Biology 14: 18-30.
736 van Etten, J.V. 2017. R package gdistance: distances and routes on geographical grids.
737 Available: https://cgspace.cgiar.org/handle/10568/83180. Accessed 1 September 2018.
738 Wagner, C.E., Keller, I., Wittwer, S., Selz, O.M., Mwaiko, S., Greuter, L., Sivasundar, A. and
739 Seehausen, O. 2013. Genome-wide RAD sequence data provide unprecedented

740 resolution of species boundaries and relationships in the Lake Victoria cichlid adaptive
741 radiation. Molecular Ecology 22: 787-798.
742 Waits, L. P., Cushman, S. A., and Spear, S. F. 2016. Applications of landscape genetics to
743 connectivity research in terrestrial animals. *In:* Landscape Genetics: Concepts, Methods,
744 Applications, First Edition. John Wiley and Sons Ltd., p. 199-219.
745 Weyer, J., Jørgensen, D., Schmitt, T., Maxwell, T. J., and Anderson, C. D. 2014. Lack of
746 detectable genetic differentiation between den populations of the Prairie Rattlesnake
747 (*Crotalus viridis*) in a fragmented landscape. Canadian Journal of Zoology 92: 837-846.
748 Wickham, J. D., Riitters, K. H., Wade, T. G., Coan, M., and C. Homer. 2007. The effect of
749 Appalachian mountaintop mining on interior forest. Landscape Ecology 22: 179-187.
750 Wickham J, Wood P.B., Nicholson M.C., Jenkins W., Druckenbrod D., Suter G.W., Mazzarella
751 C., Gallow W., and Amos, J. 2013. The overlooked terrestrial impacts of mountaintop
752 mining. BioScience 63: 335-348.
753 Willing, E. M., Dreyer, C., and Van Oosterhout, C. 2012. Estimates of genetic differentiation
754 measured by F_{ST} do not necessarily require large sample sizes when using many SNP
755 markers. PloS one 7:e42649.
756

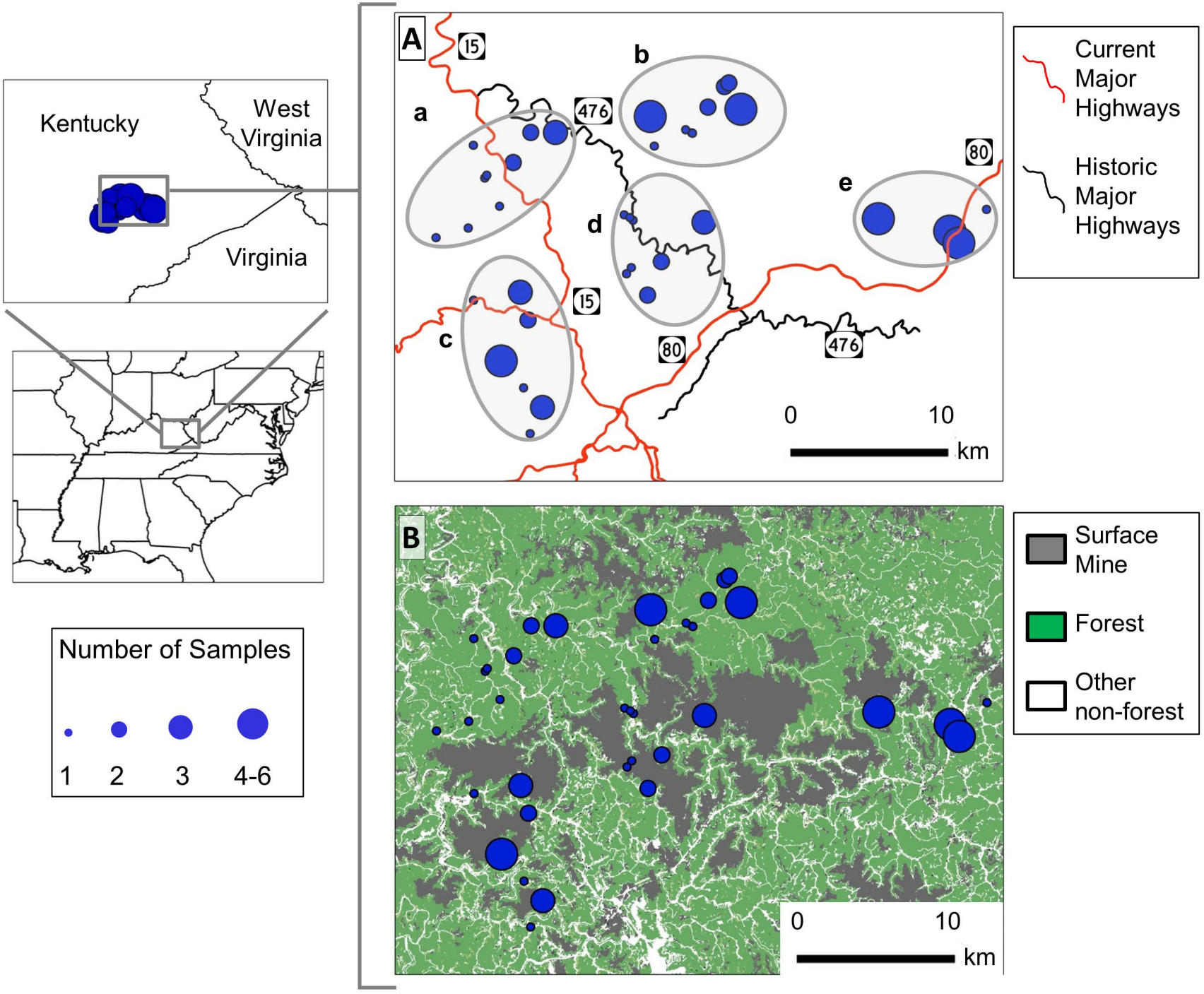
Kentucky
West Virginia
Virginia
A
15
476
80
a
b
c
d
e
0
10
km
Current Major Highways
Historic Major Highways
B
Surface Mine
Forest
Other non-forest
Number of Samples
1
2
3
4-6

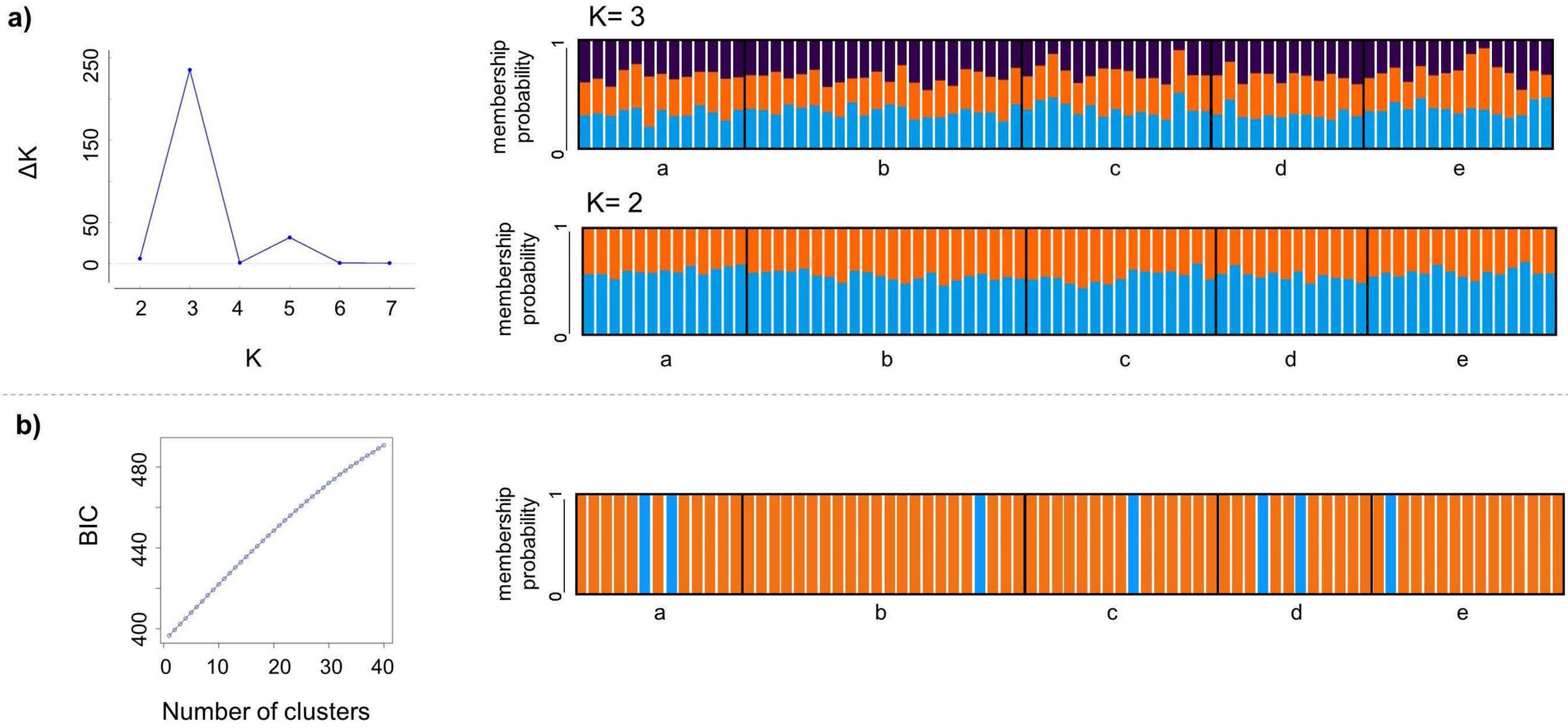
a)
ΔK
0
50
150
250
2
3
4
5
6
7
K
K= 3
membership probability
1
0
a
b
c
d
e
K= 2
membership probability
1
0
a
b
c
d
e
b)
BIC
400
440
480
0
10
20
30
40
Number of clusters
membership probability
1
0
a
b
c
d
e

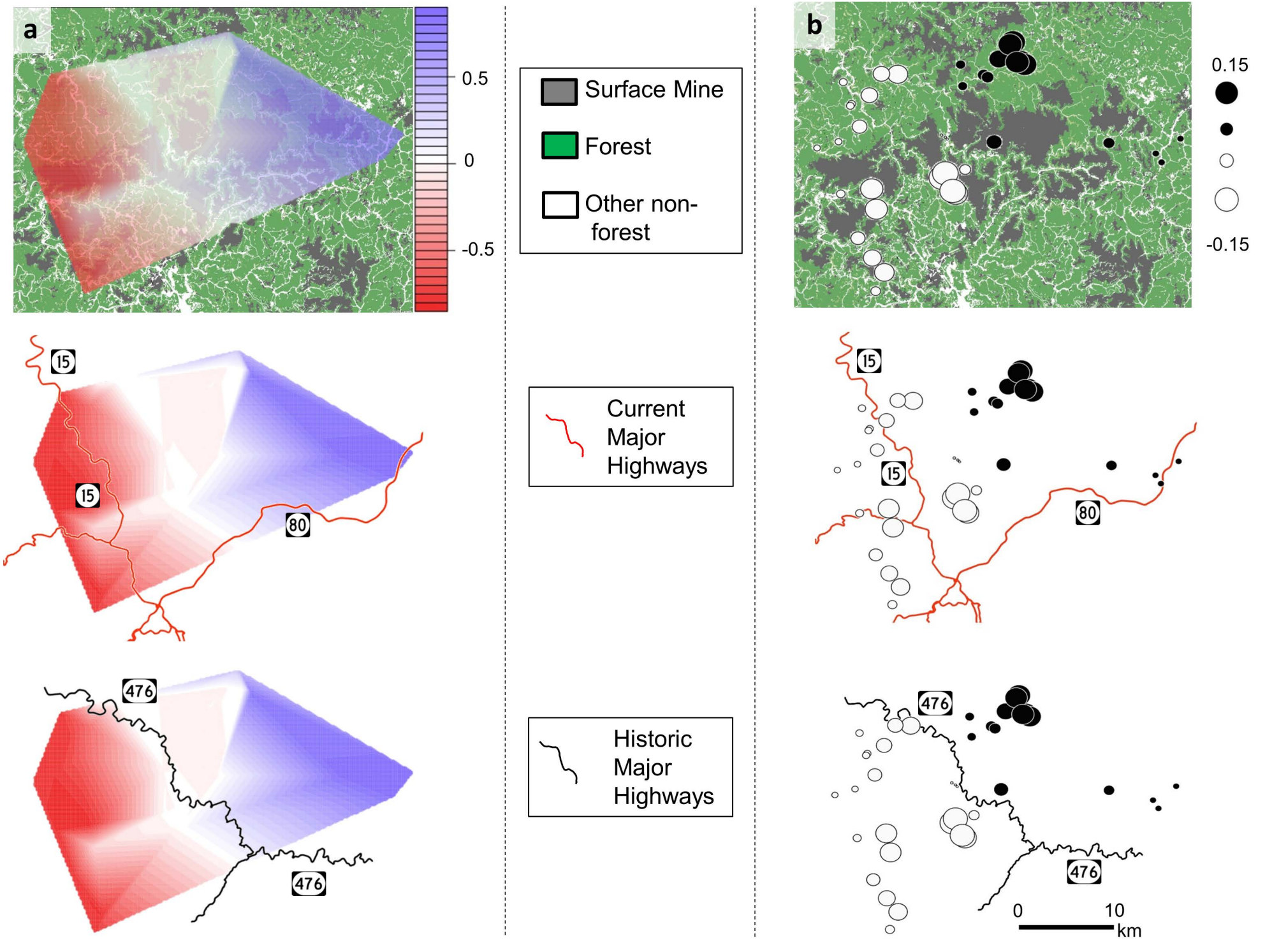
a
0.5
0
-0.5
Surface Mine
Forest
Other non-forest
b
0.15
-0.15
15
15
80
Current Major Highways
15
15
80
476
476
Historic Major Highways
476
476
0
10
km

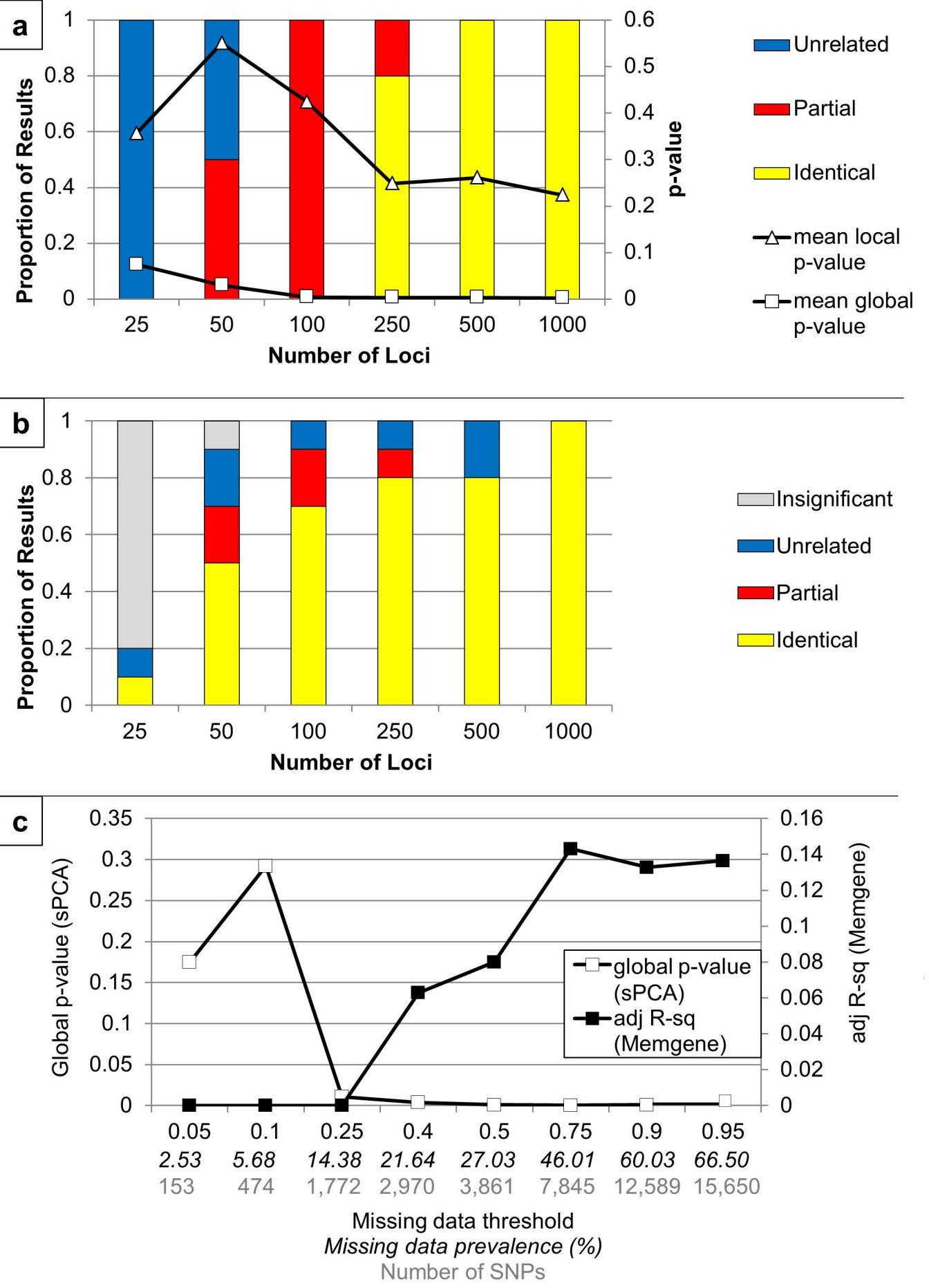
a
Proportion of Results
p-value
Number of Loci
25
50
100
250
500
1000
Unrelated
Partial
Identical
mean local p-value
mean global p-value
b
Proportion of Results
Number of Loci
Insignificant
Unrelated
Partial
Identical
c
Global p-value (sPCA)
adj R-sq (Memgene)
global p-value (sPCA)
adj R-sq (Memgene)
0.05
0.1
0.25
0.4
0.5
0.75
0.9
0.95
2.53
5.68
14.38
21.64
27.03
46.01
60.03
66.50
153
474
1,772
2,970
3,861
7,845
12,589
15,650
Missing data threshold
Missing data prevalence (%)
Number of SNPs